NASA TECHNICAL MEMORANDUM

NASA TM X-3219

NASA TM X-3219

ANALYSIS OF A STABILITY VALVE SYSTEM FOR EXTENDING THE DYNAMIC RANGE OF A SUPERSONIC INLET

John A. Webb, Jr., and Miles O. Dustin

Lewis Research Center

Cleveland, Ohio 44135

NATIONAL AERONAUTICS AND SPACE ADMINISTRATION • WASHINGTON, D. C. • MAY 1975

1. Report No. NASA TM X-3219	2. Government Accession No.	3. Recipient's Catalog No.
4. Title and Subtitle ANALYSIS OF A STABILITY VALVE SYSTEM FOR EXTENDING THE DYNAMIC RANGE OF A SUPERSONIC INLET		5. Report Date May 1975 6. Performing Organization Code
7. Author(s) John A. Webb, Jr., and Miles O. Dustin		8. Performing Organization Report No. E-8114
9. Performing Organization Name and Address Lewis Research Center National Aeronautics and Space Administration Cleveland, Ohio 44135		10. Work Unit No. 516-51 11. Contract or Grant No.
12. Sponsoring Agency Name and Address National Aeronautics and Space Administration Washington, D.C. 20546		13. Type of Report and Period Covered Technical Memorandum 14. Sponsoring Agency Code

15. Supplementary Notes

16. Abstract

A stability valve system designed for a full-scale, flight, supersonic, mixed-compression inlet was modeled dynamically by using analog computer techniques. The system uses poppet valves mounted in the inlet cowl to bypass airflow and augments the inlet shock position control system by preventing unstarts caused by high-frequency perturbations. The model was used as a design aid to investigate the effects of varying both the physical configurations of the valve and the flight and wind tunnel conditions. Results of the analysis indicate that the stability valve will provide a bandpass operation of 1 to 17 hertz.

17. Key Words (Suggested by Author(s))	18. Distribution Statement
Supersonic inlet Shock stability Inlet bleed Poppet-valve dynamics	Unclassified - unlimited STAR Category 07 (rev.)

19. Security Classif. (of this report)	20. Security Classif. (of this page)	21. No. of Pages	22. Price*
Unclassified	Unclassified	38	$3.75

* For sale by the National Technical Information Service, Springfield, Virginia 22151

ANALYSIS OF A STABILITY VALVE SYSTEM FOR EXTENDING THE DYNAMIC RANGE OF A SUPERSONIC INLET

by John A. Webb, Jr., and Miles O. Dustin

Lewis Research Center

SUMMARY

An analytical model of the dynamic performance of a stability valve system designed for a full-scale, flight, supersonic, mixed-compression inlet is presented. The stability valve system augments the inlet shock position control system by providing a high-response airflow bleed upstream of the inlet's shock trap to prevent the occurrence of inlet unstarts. The analysis presented in this report determines the pneumatic and mechanical dynamics of the poppet valves that are used to respond to increased cowl bleed pressure by opening and bypassing excess inlet airflow. The valves were simulated by using analog computer techniques as a design aid.

Two valve designs are presented. One employs a shield upstream of the valve poppet to eliminate the effect of flow forces, and the other is the basic unshielded valve. The low-frequency dynamic characteristics of the valves are altered by the addition of bleed orifices. These orifices provide a small flow path which equalizes the steady-state pressures acting on either side of the poppet. This results in a valve which has a bandpass type of operation.

Results are presented in the form of valve position responses to disturbances in shock position. The effects of disturbance size, valve configuration, and operating conditions on the valve position response were determined. The relative stability of the valve was shown to be dependent on the disturbance size. This dependence is attributed to system nonlinearities. The effect of flow forces was shown to be negligible. However, the valve configuration using the shield demonstrated additional damping as a result of the removal of the actuating pressure drop with valve opening. The effect of inlet ambient operating conditions was small for the results presented, slightly decreasing the valve's relative stability at high ambient pressures. The shielded stability valve with bleed orifices exhibited a frequency response range from about 1 to 17 hertz.

INTRODUCTION

A supersonic inlet provides subsonic airflow to an engine at as high a pressure as possible. When a portion of an inlet's supersonic area contraction is accomplished internally, it is called a mixed-compression inlet. Optimum performance of a mixed-compression inlet is obtained with the terminal shock located in the inlet throat. The position of the terminal shock is affected by the balance between the engine airflow required and the amount of airflow captured by the inlet. Airflow perturbations on either end of the inlet can cause the terminal shock to change position, resulting in suboptimal performance. If the shock moves upstream of the inlet throat, an unstable condition exists that results in the expulsion of the shock out the front of the inlet. This condition is called unstart.

Unstarts cause undesirable effects on the propulsion system and aircraft aerodynamics. Therefore, it is necessary to control the position of the terminal shock to prevent suboptimal performance and unstarts. In order to accomplish this, bypass doors are located in the subsonic portion of the inlet and are controlled to keep the terminal shock in the inlet throat by dumping excess air overboard (ref. 1). These doors require a feedback signal to indicate shock position and an electrohydraulic servosystem to actuate the doors.

This report presents the results of an analytical investigation of a stability relief valve system for augmenting existing active overboard bypass doors on a supersonic mixed-compression inlet. An analog computer simulation was used to aid in the design process by predicting the dynamic performance of the stability valve system.

The stability valve system augments the bypass door system by providing an additional cowl bleed region just upstream of the design operating point of the terminal shock. Air flows through the bleed region to a series of poppet valves located in the cowl wall. When the shock moves toward unstart, the pressure across the valve poppets increases and the valves open, dumping the bleed flow overboard. The additional bypassed airflow helps to prevent expulsion of the shock.

Previous investigations of the performance of similar stability valve systems mounted on research inlets have been reported in references 2 and 3. These systems were mounted external to the inlets and were not intended for use as flight hardware. The stability valve system analyzed in this report is designed for use on a full-scale flight inlet (ref. 1) to be tested in both wind tunnel and flight environments. The inlet has a bypass door system which is capable of responding to shock motions slower than 1 hertz. The stability relief valves are designed to improve the ability of the inlet to tolerate airflow perturbations without the occurrence of an unstart by responding to shock motions at rates beyond 10 hertz.

Two versions of the stability valve design are presented, one employing a shield to eliminate flow forces and one without the shield. These two designs were analyzed by

writing the differential equations which describe the mechanical dynamics of the system. This analysis includes nonlinear approximations to the performance of the porous cowl bleed region, the flow forces acting on the valve, and poppet friction. The flow forces and discharge coefficient of the poppet valve were determined experimentally as functions of valve position.

Data are presented in the form of valve position responses to disturbances in shock position. The effects of disturbance size, valve configuration, and operating conditions on the valve position response were determined. Ramps in shock position are shown to provide insight into the valve performance with this type of disturbance. And finally, a frequency response of the valves is presented.

STABILITY VALVE INSTALLATION

The inlet used for studying the stability valve system is an axisymmetric, mixed-compression type. It is shown in figure 1 mounted in the wind tunnel test section. A complete description of the inlet is presented in reference 4. The locations of the bypass doors and the stability valve system are shown in figure 2. As shown in the detailed sketch of the stability valves in figure 2, the porous bleed region for the valves is located just upstream of the shock trap. The inlet throat is located just downstream of the shock trap. The stability valves are mounted in two rows, with 25 valves located circumferentially around the inlet in each row. Bypassed airflow passes through the porous bleed, through the stability valve, and out through louvers, as shown by the arrows.

A more detailed view of the two versions of the stability valve is shown in figure 3. The basic valve shown in figure 3(a) is a spring-loaded poppet valve, actuated by the pressure differential of $p_b - p_c$. (The symbols used throughout the text are defined in appendix A.) The pressure above the poppet p_c is maintained at a reference value by means of a reference plenum containing pressure p_a. Pneumatic damping is provided by separating p_c from p_a with an orifice (orifice 5).

The shielded valve shown in figure 3(b) differs from the basic valve in figure 3(a) by the addition of a shield between the valve poppet and the porous bleed. The actuating pressure becomes $p_p - p_c$, where p_p is ducted from the inlet through a 2.54-centimeter-wide duct located just upstream of the shock trap. The shield was designed to eliminate the effect of flow forces on the poppet. Flow forces are caused by local high velocities of air near the valve opening, which create a decreased static pressure acting on the valve face area (ref. 5). The shield limits the area over which this force can act to the metering edge of the poppet. An additional benefit derived from the shield is the fact that p_p is not affected by a rapid opening of the valve as greatly as p_b. If p_b increases rapidly on the unshielded valve, indicating motion of the shock toward

unstart, the valve will open and the immediate flow out of volume V_b will cause a drop in p_b, which tends to reclose the valve. This type of action decreases the relative stability of the valve position. Therefore, the addition of a shield provides a stabilizing effect on the action of the valve. The gain or sensitivity of the shielded valve position to shock motion is also greater than in the unshielded valve since the pressure p_p rises much more rapidly than p_b as the shock moves upstream.

ANALYTICAL DESCRIPTION OF STABILITY VALVE SYSTEM

The stability valve system was analyzed by writing continuity and momentum equations to describe one of the 25 compartments located circumferentially behind the porous bleed region (fig. 2). Poppet valve dynamics were analyzed for one valve, and the valve flow was doubled to account for the presence of two valves in a compartment.

Bleed Region Performance

The dynamics of the inlet duct are not considered in this analysis. Instead, the input to the system is shock position and the porous bleed flow is determined from shock position x_s and downstream pressure on the bleed p_b. A plot of normalized mass flow $\dot{m}_b$ entering the cowl bleed from the subsonic region against load pressure is presented in figure 4 with lines of constant shock position. These curves were estimated from data on porous bleed performance of previously tested inlets as presented in reference 3. Airflow was also assumed to enter the bleed region from the supersonic area upstream of the shock. This flow is designated $\dot{m}_{ss}$ (fig. 3(a)) and is approximated by

$$\dot{m}_{ss} = B(X_b - x_s)(P_{ss} - p_b) \tag{1}$$

where P_{ss} is the average static pressure upstream of the terminal shock. The preceding equation assumes the supersonic bleed flow to be proportional to the product of the bleed region in supersonic flow and the pressure differential across the bleed. The supersonic bleed flow may be negative, indicating some recirculating flow around the terminal shock.

Valve Flow Forces and Discharge Coefficient

The flow forces and discharge coefficient for the poppet valve were determined experimentally as a function of valve position. The experiment was conducted with a

1/6th-scale model of the poppet as described in appendix B. The results of the flow force determination are shown in figure 5. In order to eliminate the effect of upstream pressure, the flow force was normalized by dividing F_{fl} by p_b. A curve was drawn through the data points for use in the analog computer analysis.

The discharge coefficient of the poppet valve for choked flow is plotted in figure 6. Experimental data were obtained for two upstream pressures and two seat configurations (round and square edge). For analysis purposes this result can be approximated by a straight line of the form

$$C_v = C_{vc} - ax_v \tag{2}$$

where C_v is the poppet valve discharge coefficient, C_{vc} is the intercept of the line in figure 6 at valve closure, and a is the slope of that line.

Dynamics of Unshielded Valve

The mechanical dynamics of the unshielded stability valve were determined by summing the forces acting on the poppet (fig. 3).

$$M_p\ddot{x}_v + K_{sp}x_v + F_{sp} + F_{fl} - (p_b - p_c)A_p + F_r = 0 \tag{3}$$

The initial spring force is designated F_{sp}. Friction force F_r is treated as static friction, where F_r is constant and has the same sign as the poppet velocity $\dot{x}_v$.

The pressure in the volume behind the porous bleed was determined by summing flows and applying the continuity equation

$$\dot{p}_b = \frac{\gamma RT}{V_b}(\dot{m}_b + \dot{m}_{ss} - 2\dot{m}_v - 2\rho_b A_p \dot{x}_v) \tag{4}$$

The two bleed region flows $\dot{m}_b$ and $\dot{m}_{ss}$ are defined by figure 4 and equation (1), respectively. The flow through the poppet valve $\dot{m}_v$ was doubled to account for the presence of two valves (fig. 2). Assuming that the valve is choked,

$$\dot{m}_v = \frac{C_v C_g \pi D_v x_v p_b}{\sqrt{T}} \tag{5}$$

where

$$C_g = \sqrt{\frac{\gamma g_c}{R}\left(\frac{2}{\gamma+1}\right)^{(\gamma+1)/(\gamma-1)}} = 0.0405 \frac{kg\sqrt{K}}{(N)(sec)} \tag{6}$$

for an isentropic process and C_v is the valve discharge coefficient which is described by equation (2). The term $2\rho_b A_p \dot{x}_v$ in equation (4) accounts for the volume of fluid displaced by the motion of the two poppets.

A similar equation can be written for the pressure above the poppet in volume V_c

$$\dot{p}_c = \frac{\gamma RT}{V_c}(\rho_c A_p \dot{x}_v - \dot{m}_5) \tag{7}$$

In this case the volume V_c is sufficiently small with respect to the volume displaced by the poppet that it must vary with valve motion.

$$V_c = V_{cc} - A_p x_v \tag{8}$$

The flow out of volume V_c is through the damping orifice (orifice 5).

$$\dot{m}_5 = C_d A_5 \sqrt{2g_c \rho_c}\sqrt{p_c - p_a} \tag{9}$$

The discharge coefficient for this and all unchoked orifices is assumed to be 0.6.

The pressure in the reference volume is

$$\dot{p}_a = \frac{\gamma RT}{V_a}\dot{m}_5 \tag{10}$$

assuming no leakage.

Dynamics of Shielded Valve

The addition of the shield alters the dynamics of the system. The summation of the forces acting on the poppet remains essentially the same as equation (1), except that p_b is replaced by p_p and $F_{fl} = 0$. That is,

$$M_p \ddot{x}_v + K_{sp} x_v + F_{sp} - (p_p - p_c)A_p + F_r = 0 \tag{11}$$

The pressure in volume V_p is found from

$$\dot{p}_p = \frac{\gamma RT}{V_p} (\dot{m}_6 - \rho_p A_p \dot{x}_v) \tag{12}$$

where

$$\dot{m}_6 = C_d A_c \sqrt{2 g_c \rho_d} \sqrt{p_d - p_p} \tag{13}$$

The pressure p_d in the tube which supplies the shield reflects the inlet duct pressure at the downstream end of the bleed region. Since the resistance to airflow entering the tube is small, tube dynamics can be neglected. The pressure in the tube is approximated by

$$p_d = P_{ss} + bP_0 x_s \qquad \text{for } 0 < x_s < 2.54 \text{ cm} \tag{14}$$

where P_{ss} is the average static pressure upstream of the terminal shock and bP_0 is the sensitivity of p_d to shock position as determined from inlet pressure profiles across the terminal shock. Shock position affects p_d only for the 2.54 centimeters of motion required to traverse the shield tube opening. For any motion beyond 2.54 centimeters, p_d is assumed to be at the pressure level which occurs in the inlet downstream of the shock.

One additional change created by addition of the shield is that the piston no longer displaces fluid from volume V_b. This changes equation (4) to

$$\dot{p}_b = \frac{\gamma RT}{V_b} (\dot{m}_b + \dot{m}_{ss} - 2\dot{m}_v) \tag{15}$$

The remaining portions of the shielded-valve system are the same as those without the shield and are described by equations (5) to (10).

Addition of Bleed Orifices

The previously described analysis assumes that there is no leakage either around the poppet piston or in or out of the reference volumes. However, in order to alter the low-frequency performance of the valve, some flow paths are created by introducing orifices 1 to 4, as shown in figure 7(a). This analysis is presented for only the shielded valve. The addition of bleed orifices to the unshielded valve can be analyzed in a similar manner.

Orifices 2 to 4 provide parallel flow paths from V_p to V_c. This allows p_c to track slow changes in p_p, thus preventing steady-state changes from opening the valve.

The effective orifice area is a function of valve position and is plotted in figure 7(b). When the valve is closed, orifices 2 and 3 are effective, providing the largest flow path to prevent small transients and pressure disturbances from cracking the valve. For the case when a large transient opens the valve almost full open, orifices 3 and 4 are effective, providing sufficient flow area to gradually close the valve in the event of a sustained disturbance. When only orifice 3 is open, the valve is partially open; and the flows through orifices 1 and 3 should be nearly balanced to prevent the valve from moving. Orifice 1 is provided to bleed flow out of volume V_a to keep the steady-state pressure p_a less than p_c.

The overall effect of the bleed orifices is to cause the reference pressure p_c to adjust to changing steady-state conditions. This puts a low-frequency cutoff on the valve's frequency response. The stability valve then would respond only to rapid changes in shock position (high-frequency airflow perturbations). The bypass door system would respond to slower changes. Thus, the stability valves augment the existing bypass door control system to extend the high-frequency performance of the inlet's shock position control.

Addition of the bleed orifices on the shielded valve is accomplished analytically by adding bleed orifice flows to the existing equations. Equation (12) becomes

$$\dot{p}_p = \frac{\gamma RT}{V_p} (\dot{m}_6 - \rho_p A_p \dot{x}_v - \dot{m}_t) \tag{16}$$

where

$$\dot{m}_t = C_d A_t \sqrt{2 g_c \rho_p} \sqrt{p_p - p_c} \tag{17}$$

and A_t is defined by figure 7(b). Also equation (7) becomes

$$\dot{p}_c = \frac{\gamma RT}{V_c} (\rho_c A_p \dot{x}_v - \dot{m}_5 + \dot{m}_t) \tag{18}$$

and equation (10) becomes

$$\dot{p}_a = \frac{\gamma RT}{V_a} (\dot{m}_5 - \dot{m}_1) \tag{19}$$

where

$$\dot{m}_1 \doteq \frac{C_d C_g \pi D_1^2 p_a}{4\sqrt{T}} \tag{20}$$

assuming orifice 1 to be choked. These equations are applied to the shielded valve model to determine the performance of the bleed orifice system.

SIMULATION RESULTS AND DISCUSSION

The preceding equations were simulated by using the analog simulation described in appendix C. This simulation was used as a design aid to determine the relative stability of each valve configuration. It also was useful for evaluating the effect of varying ambient conditions on the valve's relative stability. Most of the data presented herein are in the form of valve position responses to a step in shock position as recorded on a strip-chart recorder. Additional results are provided to show the response of the valve position to both ramp and small-amplitude sinusoidal inputs in shock position. The physical constants used to obtain these data are listed in table I.

Unshielded Valve Without Bleed Orifices

Figure 8 shows a typical recording of simulation signals when the unshielded valve was used. Shock position was stepped 5 centimeters upstream, which caused an immediate rise in p_b, thus opening the valve and increasing bleed mass flow $\dot{m}_b$. The initial spike on $\dot{m}_b$ occurs because the step input in shock position is instantaneous and moves the operating point on figure 4 parallel to the $\dot{m}_b/\dot{M}_0$ axis since p_b cannot respond instantaneously.

The effect of changing the damping orifice diameter and the static friction force on the valve position response is shown in figure 9. The response can be changed from relatively underdamped with a large overshoot and undershoot as in the upper left trace to highly damped as in the lower right trace. Use of the smallest damping orifice size (D_5 = 0.508 cm) appears to result in a small oscillation near the valve's final position and near closure. From this figure a valve damping orifice diameter of 0.762 centimeter and a friction of 6.68 newtons were selected to obtain a valve with no overshoot. When this valve is subjected to various step sizes, the nonlinearities of the system affect the valve's relative stability, as shown in figure 10. The valve overshoots on opening for small steps and exhibits a small oscillation near closure for large steps.

In order to determine the effect of flow forces on the poppet valve response independent of other effects, a test was run on the unshielded valve with and without flow forces. This eliminated the additional changes in the system which occur when the shield is added to the valve. Results of this test are shown in figure 11 for two different valve configurations. Although the steady-state position of the valve is affected, the flow forces do not change the relative stability of the valve significantly.

An additional effect which should be considered is that of changing ambient conditions. Two cases for both wind tunnel and flight conditions were chosen which correspond to different altitudes at Mach 2.5. The effect of changing from one condition to another on the step response of the unshielded valve is shown in figure 12. Little change in response is seen with the exception of the high-pressure (P_0 = 11.9 N/cm^2) case for flight, where the valve responds slightly faster than for the other cases.

Shielded Valve Without Bleed Orifices

When the shield is added to the valve, the step response varies with friction and damping orifice diameter, as shown in figure 13. In comparison to figure 9, the shield adds a considerable amount of damping. Therefore, the largest possible damping orifice diameter and smallest amount of friction were selected for the following studies. Figure 14 shows that step size changes do not affect the shielded-valve response.

As in the case of the unshielded valve, wind tunnel and flight condition changes affect the valve only for the high-pressure flight condition, as shown in figure 15. At this condition the valve becomes somewhat underdamped, indicating a tendency towards less stability at higher pressures.

Frictionless Operation

Both shielded and unshielded valves were tested with friction removed, as shown in figure 16. The unshielded valve resonated at 23 hertz, and the shielded valve resonated at 12 hertz. The oscillations of the unshielded valve decayed more rapidly because of the smaller damping orifice size selected for this valve.

Addition of Bleed Orifices to Shielded Valve

The addition of bleed orifices has little effect on the step response of the valve, but they do change its low-frequency characteristics. The effect of adding orifice 3 is shown in figure 17(a). The airflow across the piston allows p_c to increase, closing the valve at a rate of about 1 cm/sec. When orifice 1 is included (fig. 17(b)), the flows of the two orifices eventually balance, and the poppet remains open as long as the disturbance persists.

When all bleed orifices are included, the valve responds as shown in figure 18. For a shock position step of 0.508 centimeter, the stability valve does not move since the pressure rise in p_p is insufficient to overcome the closed spring force on the poppet.

The stability valve does respond, however, to a step in shock position of 0.762 centimeter. In this case, orifice 2 is closed as the valve opens; and the valve remains open since orifice 1 and 3 flows are balanced. Increasing the input step size to 1.02 centimeters drives the valve far enough to open orifice 4, which bypasses airflow around the poppet, thus increasing p_c and closing the valve. The closure rate again is roughly 1 cm/sec since orifice 4 has the same area as orifice 3. The valve closes until orifice 4 is closed off and a bleed flow balance is established. For step inputs of shock position greater than 1.02 centimeters the valve behaves in a similar manner, except for the addition of a delay time during which the valve remains fully open until pressure p_c is raised high enough to start motion towards closure.

The effect of shock motion at a constant velocity is demonstrated in figure 19 for various rates of shock motion across the shield tube entrance. For shock velocities of 2.6 cm/sec or less the valve will not respond. At a shock velocity of 2.7 cm/sec the valve opens slightly after the shock passes 2 centimeters of motion and quickly closes because orifice 2 has not been closed. When the velocity is raised to 2.9 cm/sec, the valve opens sufficiently to open orifice 4, and at a velocity of 3.2 cm/sec the valve is driven fully open. The cowl subsonic porous bleed flow $\dot{m}_b$ shown in figure 19 indicates that some flow is entering into the bleed region when the valve is closed. This flow is the charging flow into volume V_b.

Frequency Responses of Stability Valves

In order to further demonstrate the response capabilities of the valves and the low-frequency effects of the bleed orifices, frequency responses of valve position to shock position were obtained for the unshielded and shielded valves. These responses were obtained (1) with no bleed orifices, (2) with orifice 3, and (3) with orifices 2 and 3. All responses were normalized to the 1-hertz amplitude of the response with no bleed orifices. The unshielded-valve response was obtained with a 2.54-centimeter zero-to-peak sinusoidal shock motion, and the shielded-valve response with a 0.254-centimeter zero-to-peak sinusoidal input. These disturbance sizes were selected to provide a valve motion of 0.25 centimeter zero to peak.

The response of the unshielded valve is shown in figure 20(a). The effect of increasing bleed orifice area is to decrease the operating bandwidth of the valve on the low-frequency end. This low-frequency response ranges from a corner (-3 dB) at 0.2 hertz for orifice 3 only to a corner at 2 hertz for orifices 2 and 3. The unshielded valve exhibits a resonant characteristic at about 12 hertz and a high-frequency corner (-3 dB) at 30 hertz. The addition of the shield to the stability valve (fig. 20(b)) further decreases the system bandwidth, with a low-frequency cutoff (-3 dB) at 0.6 to 2.4 hertz depending on which orifices are active and a high-frequency response which is down 3 decibels at

17 hertz. The shielded valve resonates at 9 hertz with an amplitude of 6 to 8 decibels. A comparison of figures 20(a) and (b) shows that the shielded valve is somewhat more resonant than the unshielded valve. Also the addition of orifice 2 appears to diminish the amplitude of response over most frequencies.

CONCLUDING REMARKS

An analytical model of a stability valve system for use on an axisymmetric, mixed-compression, supersonic inlet is presented. The model includes valve system dynamics and is intended to aid in the design process and to predict the relative stability of the system. An analog computer was used to demonstrate the effects of (1) friction, (2) damping orifice size, (3) shock position step size, (4) flow forces, (5) addition of a shield to the valve poppet, (6) different altitude conditions for wind tunnel and flight performance, and (7) the addition of bleed orifices to alter the valve's frequency response.

Results demonstrate that the relative stability of the unshielded valve can be adjusted by using a pneumatic damping orifice and poppet static friction. However, this relative stability is dependent on the amplitude of the shock position step disturbances. The amplitude dependence is attributed to system nonlinearities.

The effect of flow forces on the unshielded valve was shown to be negligible. Addition of a shield upstream of the poppet adds damping to the system by removal of the drop in driving pressure with valve opening. Since flow forces are negligible on the unshielded valve, the shield does not make any performance improvements as a result of removal of flow forces.

The performance of these valves is affected by ambient inlet operating conditions. Data for different altitudes at Mach 2.5 show that the valve is slightly more resonant (or less damped) for the high-pressure case corresponding to low-altitude flight. Although the changes were not great for the data shown, more extreme changes in conditions could cause undesirable valve system resonances.

The addition of bleed orifices can be used to maintain the reference pressure behind the poppet valve at steady-state operating values. This results in a valve which is responsive for a desired bandwidth of frequencies. The stability valves, therefore, can be made to respond to high-frequency perturbations, while the inlet bypass door system handles the lower frequency requirements. The shielded valve system with bleed orifices exhibits a small-amplitude frequency response which is down 3 decibels at 17 hertz with a resonance of 6 to 8 decibels at 9 hertz and a low-frequency cutoff of -3 decibels at 0.6 to 2.4 hertz depending on the orifices which are active. The stability valves with bleed orifices do not open for shock velocities of less than 2.6 cm/sec upstream.

The overall results presented in this report demonstrate the need to compromise the stability valve system performance design to provide stable valve operation over a wide range of conditions. Additional considerations such as coupling effects between the valves and other inlet controls or bleed systems, drag effects caused by dumping flow directly overboard, and the effect of aircraft acceleration loading have not been considered in this analysis and may be significant enough to warrant further investigation.

Lewis Research Center,
National Aeronautics and Space Administration,
Cleveland, Ohio, January 17, 1975,
516-51.

APPENDIX A

SYMBOLS

A	area, cm^2
a	slope of variable discharge coefficient curve, 1/cm
B	supersonic bleed flow gain, (cm)(kg)/(N)(sec)
b	slope of shield tube pressure, 1/cm
C	coefficient
C_g	coefficient for orifice equation (see eq. (6)), (kg)($\sqrt{K}$)/(N)(sec)
D	diameter, cm
F	force, N
g_c	gravitational constant, 100 (kg)(cm)/(N)(sec^2)
K	spring rate, N/cm
M	mass, kg
$\dot{M}$	constant mass flow rate, kg/sec
$\dot{m}$	dynamic mass flow rate, kg/sec
P	constant pressure, N/cm^2 abs
P_{ss}	average static pressure upstream of terminal shock, N/cm^2 abs
p	dynamic pressure, N/cm^2 abs
R	universal gas constant, 28 700 (cm)(N)/(K)(kg)
Re	Reynolds number
T	temperature, K
V	volume, cm^3
v	velocity, cm/sec
X	total length, cm
x	position, cm
Δx	amplitude of step in position, cm
γ	ratio of specific heats, 1.4
ρ	mass density, kg/cm^3
μ	viscosity, (N)(sec)/cm^2

Subscripts:

a	reference volume a
atm	atmospheric
b	cowl bleed, refers to volume b downstream of porous bleed
c	volume c above poppet
cc	volume c at valve closure
d	discharge
f	full scale
fl	flow
m	scaled model
p	poppet, refers to volume p between poppet and shield
r	friction
s	shock
sp	spring
ss	supersonic
t	total of bleed orifices 2, 3, and 4
v	valve
vc	discharge at valve closure
0	free-stream total
1, 2, 3, 4, 5, 6	numbered orifices (fig. 7(a))

APPENDIX B

SCALE MODEL FOR DETERMINING POPPET CHARACTERISTICS

The performance of a poppet-type valve as used for the inlet stability valve system can exhibit dynamic instabilities caused by flow forces acting on the valve (ref. 5). These forces are somewhat dependent on the poppet and seat design. Since the possibility of instabilities existed for this system, it was necessary to determine an estimate of flow forces experimentally during the initial design phase of the program. For the sake of time, convenience, and cost, a scale model of the valve poppet was flow tested to determine the magnitude of the flow forces and the valve discharge coefficient.

The valve was modeled by matching Reynolds number and Mach number as discussed in reference 6. That is,

$$\mathrm{Re} = \frac{\rho_f D_f v_f}{\mu_f} = \frac{\rho_m D_m v_m}{\mu_m} \tag{B1}$$

and

$$\text{Mach number} = \frac{v_f}{\sqrt{\gamma R T_f}} = \frac{v_m}{\sqrt{\gamma R T_m}} \tag{B2}$$

The density term in equation (B1) can be expressed as

$$\rho = \frac{P}{RT} \tag{B3}$$

where densities and pressures are considered to be just upstream of the valve. By combining equations (B1) to (B3), a relationship for the physical size ratio of the model is found as a function of other scaling ratios,

$$\frac{D_f}{D_m} = \left(\frac{P_m}{P_f}\right)\left(\frac{\mu_f}{\mu_m}\right)\sqrt{\left(\frac{T_f}{T_m}\right)} \tag{B4}$$

where the physical dimension D is poppet diameter.

For a model temperature of 20° C (293 K) and a full-scale operating temperature of 100° C (373 K), the viscosities of air are (ref. 7)

$$\mu_m = 1.81 \times 10^{-9} \text{ (N)(sec)/cm}^2$$

$$\mu_f = 2.18 \times 10^{-9} \text{ (N)(sec)/cm}^2$$

This gives a sizing ratio of

$$\frac{D_f}{D_m} = 1.36 \frac{P_m}{P_f} \tag{B5}$$

In order to assume choked flow in a model with the low-pressure side of the valve at atmospheric pressure,

$$P_m > \frac{10.1}{0.528} \text{ N/cm}^2 = 19.2 \text{ N/cm}^2 \tag{B6}$$

Assuming that the model operating at 20.7 N/cm^2 is equivalent to the full-scale valve operating at 4.8 N/cm^2 results in a scale factor D_f/D_m of 5.87. Choosing a D_f/D_m of 6 and using the temperature previously stated results in the following scaling ratio relations:

$$\frac{D_f}{D_m} = 6 \tag{B7}$$

$$\frac{A_f}{A_m} = 36 \tag{B8}$$

$$\frac{P_f}{P_m} = 0.226 \tag{B9}$$

$$\frac{F_f}{F_m} = 8.14 \tag{B10}$$

$$\frac{\dot{m}_f}{\dot{m}_m} = 7.2 \tag{B11}$$

These ratios can then be used to convert data obtained on a 1/6th-scale model of the stability valve to values for the full-scale valve.

The test stand used to test the stability valve model is shown in figure 21. The valve poppet was supported on the arm of a load cell to measure the force acting on the poppet. Linear ball bushings were used to provide smooth, stable positioning of the poppet - load-cell assembly. Air at 70 N/cm^2 was valved to supply an upstream pressure on the poppet. A pitot tube was located in the pipe for upstream total pressure measurements. An orifice plate was used to provide a valve seat to facilitate changing from a square-edged seat to a round-edged seat (used to simulate a bellmouth entrance).

The results obtained with this test are presented in figures 5 and 6. The flow forces acting on the valve were determined by measuring the total force acting on the poppet for various poppet positions and subtracting the force which existed when the valve was closed. This was done for three different upstream pressures, resulting in three curves for flow force. In order to normalize the pressure effects, the flow forces were divided by upstream pressure, resulting in the data points shown in figure 5. These data, of course, were corrected by using the modeling scale factors.

The discharge coefficient of the valve was determined by solving equation (5) of the main text for C_v and substituting measured values of mass flow $\dot{m}_v$ and upstream pressure p_b at various valve positions. The mass flow was measured by using a linear calibrated pressure drop device in the pressure supply line. Data were obtained for two upstream pressures with both a square-edged seat and a round-edge seat. These data demonstrate that the discharge coefficient does change considerably with valve opening. Values of flow coefficients less than 0.6 may be attributable to inertial effects created by the cylindrical design of the poppet.

APPENDIX C

ANALOG SIMULATION

The equations in the text were implemented on an analog computer to provide a solution for pressures, flows, and valve position as functions of time for inputs of shock position. A simplified schematic of the simulation is provided in figure 22. The nonlinear relationships of $\dot{m}_b/(\dot{M}_0 x_s)$ against p_b/P_0, F_{fl}/p_b against x_v, and A_t against x_v were generated by using diode function generators (DFG's). A feedback limiter was used to limit p_d for shock positions x_s exceeding 2.54 centimeters in order to satisfy the requirements of equation (14). The static friction force acting on the poppet was simulated by using a high-gain limiter which switched from positive to negative limits as the input went through zero.

This simulation can model either the unshielded or shielded valve with or without bleed orifices. The relays, R1 to R4, were used to change from the unshielded (-) valve model to the shielded (+) valve model. The coils to these relays are connected in parallel to a common switch to provide a single switching operation for changing models. The bleed orifice equation modifications and additions were accomplished with switches S1 and S2. Switch S1 was closed to provide bleed orifice 1, and switch S2 was closed to provide bleed orifices 2 to 4 as scheduled by valve position.

Integrators 1 to 4 were used to solve the pneumatic dynamics of equations (4) or (15), (12) or (16), (7) or (18), and (10) or (19), respectively. Integrators 5 and 6 were used to solve the mechanical valve dynamic relationships of equation (3) or (11). A comparator and logic circuit was used for the position limiter on x_v. This circuit limits x_v between 0 and 2.03 centimeters by rapidly opening an electronic switch to drop $\dot{x}_v$ coming into integrator 6 to zero. In order to provide a smooth transition coming off the limit, the initial conditions (zero output) of integrator 5 were applied to the integrator capacitor while position was limited.

REFERENCES

1. Neiner, George H.; Arpasi, Dale J.; and Dustin, Miles O.: Wind-Tunnel Evaluation of YF-12 Aircraft Inlet Control System by Frequency-Response and Transient Testing. NASA TM X-3142, 1975.

2. Sanders, Bobby W.; and Mitchell, Glenn A.: Increasing the Stable Operating Range of a Mach 2.5 Inlet. AIAA Paper 70-686, June 1970.

3. Sanders, Bobby W.; and Mitchell, Glenn A.: Throat-Bypass Bleed Systems for Increasing the Stable Airflow Range of a Mach 2.50 Axisymmetric Inlet With 40 Percent Internal Contraction. NASA TM X-2779, 1973.

4. Lewis Research Center: Wind-Tunnel Installation of Full-Scale Flight Inlet of YF-12 Aircraft for Steady-State and Dynamic Evaluation. NASA TM X-3138, 1974.

5. Tsai, D. H.; and Cassidy, E. C.: Dynamic Behavior of a Simple Pneumatic Pressure Reducer. J. Basic Eng., vol. 83, Sec. D, no. 2, June 1961, pp. 253-264.

6. Albertson, M. L.; Barton, J. R.; and Simons, D. B.: Fluid Mechanics for Engineers. Prentice-Hall, 1960, pp. 487-508.

7. Sears, Francis W.; and Zemansky, Mark W.: University Physics. Addison-Wesley, 1964, p. 320.

TABLE I. - PHYSICAL VALUES USED FOR

STABILITY VALVE SIMULATION

Poppet area, A_p, cm^2	62
Orifice 1 area, A_1, cm^2	0.0077
Orifice 6 area, A_6, cm^2	2.54
Discharge coefficient rate of change, a, 1/cm	0.146
Supersonic bleed flow gain, B, (cm)(kg)/(N)(sec)	2.04×10^{-3}
Slope of shield tube pressure, b, 1/cm	0.091
Orifice discharge coefficient, C_d	0.6
Discharge coefficient of closed poppet valve, C_{vc}	0.85
Poppet valve diameter, D_v, cm	8.89
Initial spring force, F_{sp}, N	13.3
Spring rate, K_{sp}, N/cm	3.5
Poppet mass, M_p, kg	0.20
Average static pressure upstream of terminal shock, P_{ss}	0.308 P_0
Volume a, V_a, cm^3	1.64×10^3
Volume b, V_b, cm^3	857
Volume c at valve closure, V_{cc}, cm^3	161
Volume p, V_p, cm^3	60.4
Total length of porous bleed, X_b, cm	25.4
Density, ρ	$P_0/2RT$
Free-stream total pressure, P_0, N/cm^2	[a]5.15
Free-stream total temperature, T_0, K	[a]311

[a]For all data except figs. 11 and 14.

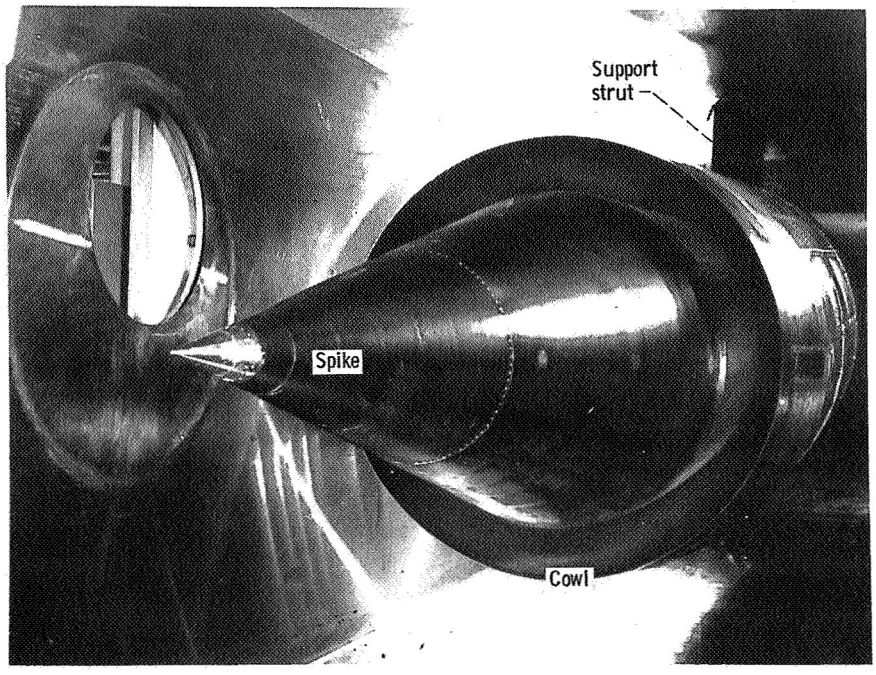

Figure 1. - Supersonic inlet used for stability valve studies, shown mounted in test section of wind tunnel.

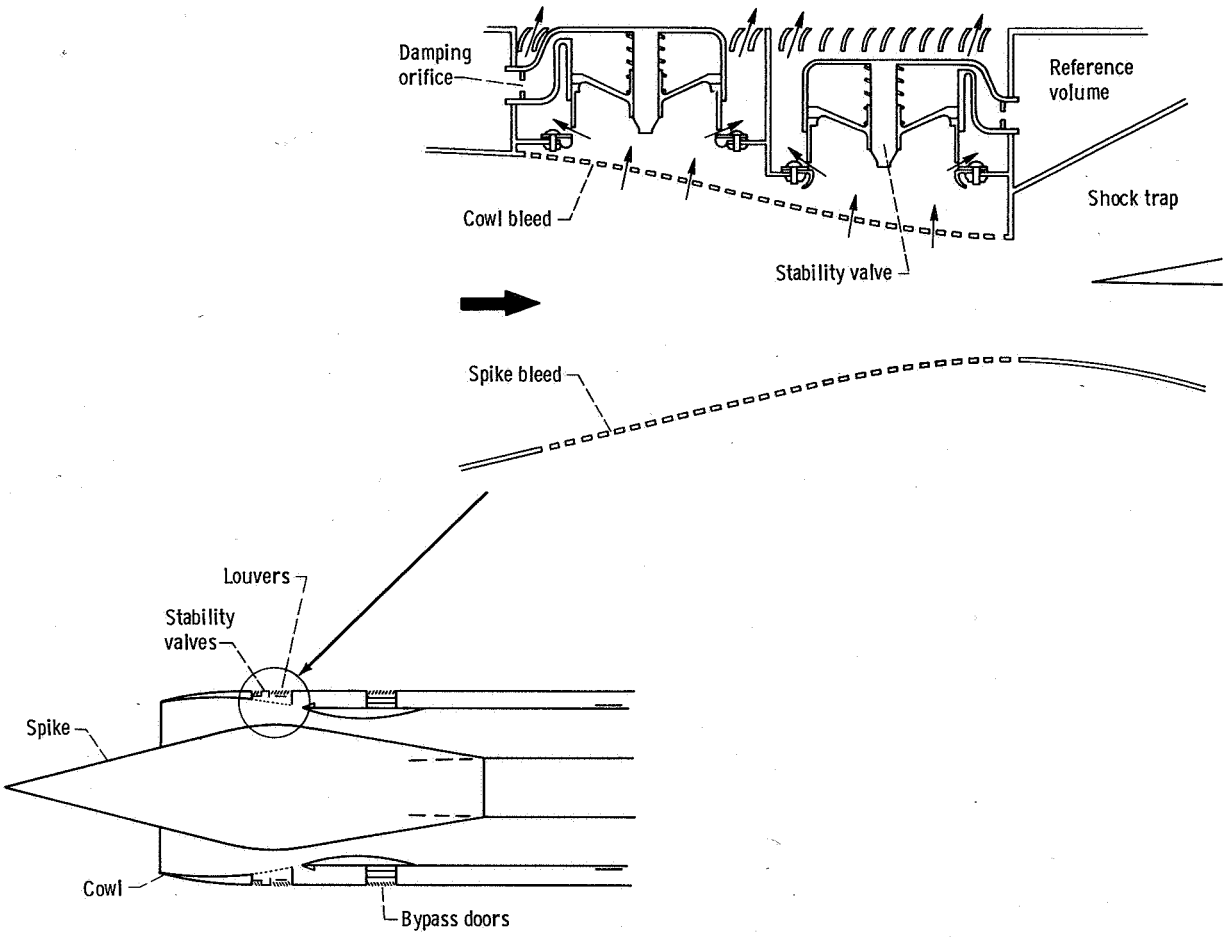

Figure 2. - Inlet configuration showing detail of stability valve installation.

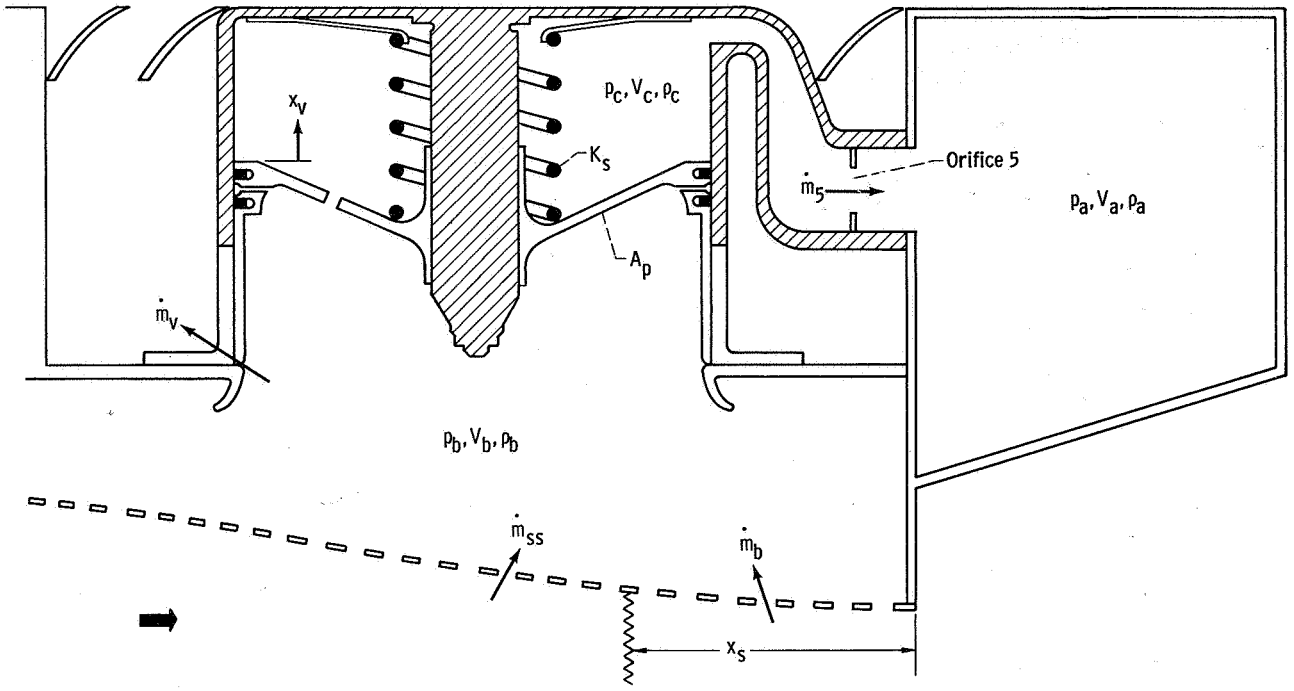

(a) Basic stability valve.

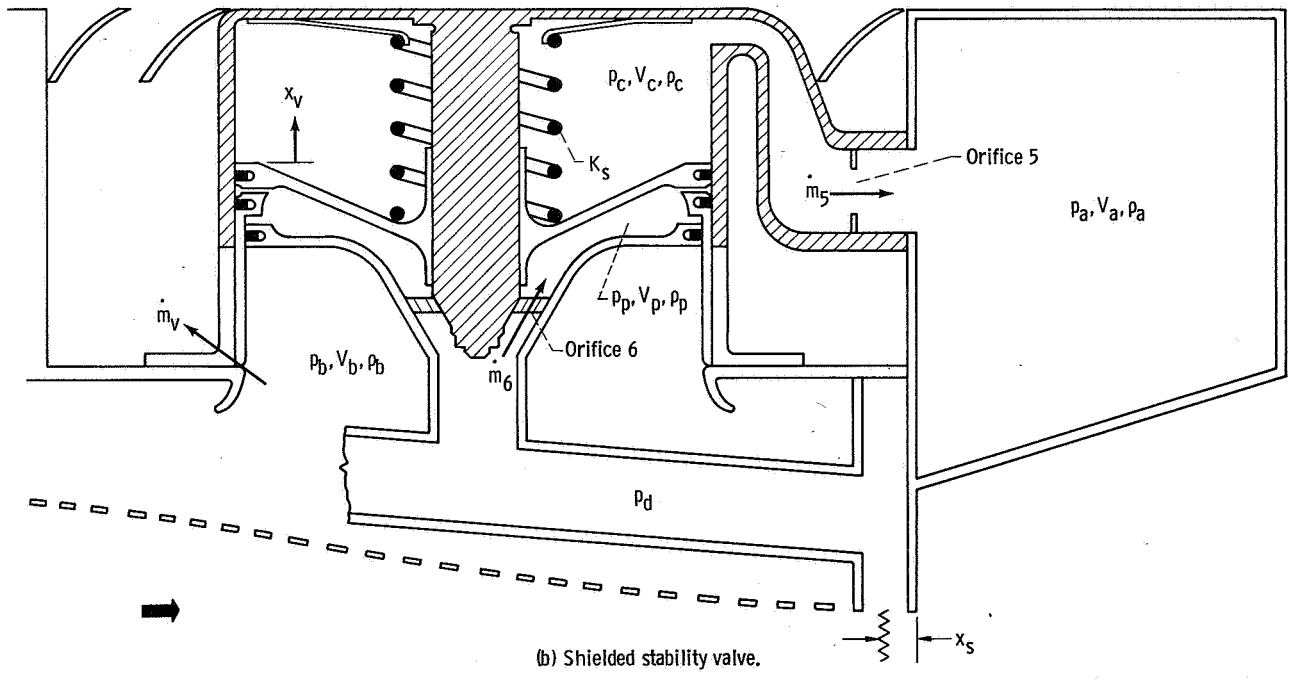

(b) Shielded stability valve.

Figure 3. - Details of stability valve design.

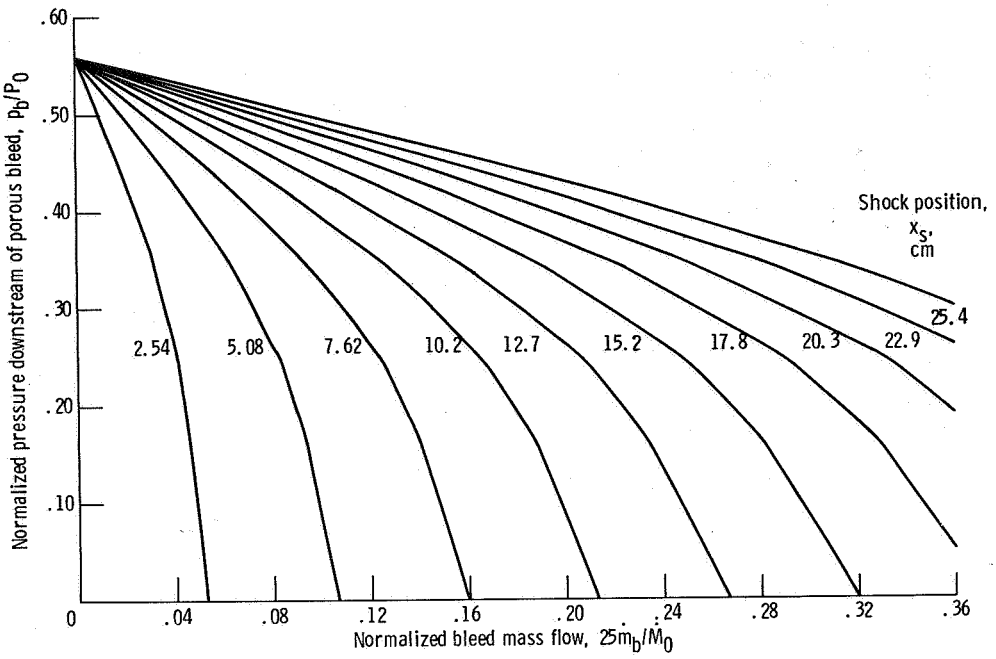

Figure 4. - Cowl bleed performance curves.

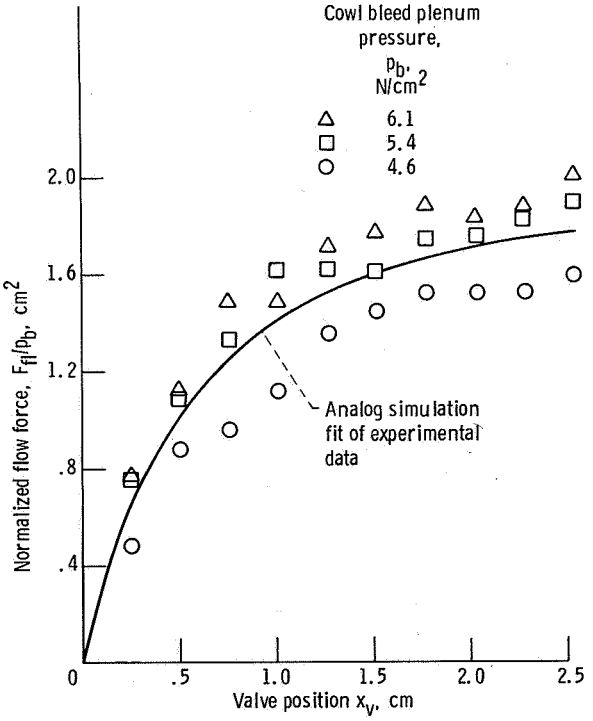

Figure 5. - Experimentally determined flow force acting on choked cylindrical poppet valve. (Data obtained from 1/6th-scale model and corrected to full scale.)

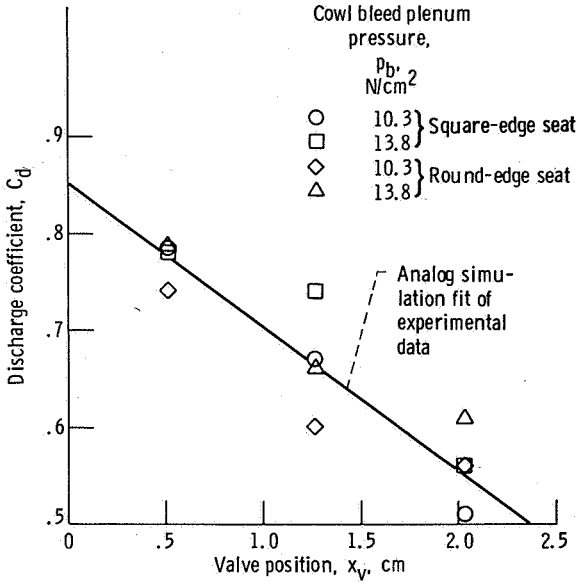

Figure 6. - Experimentally determined discharge coefficients for choked cylindrical poppet valve.

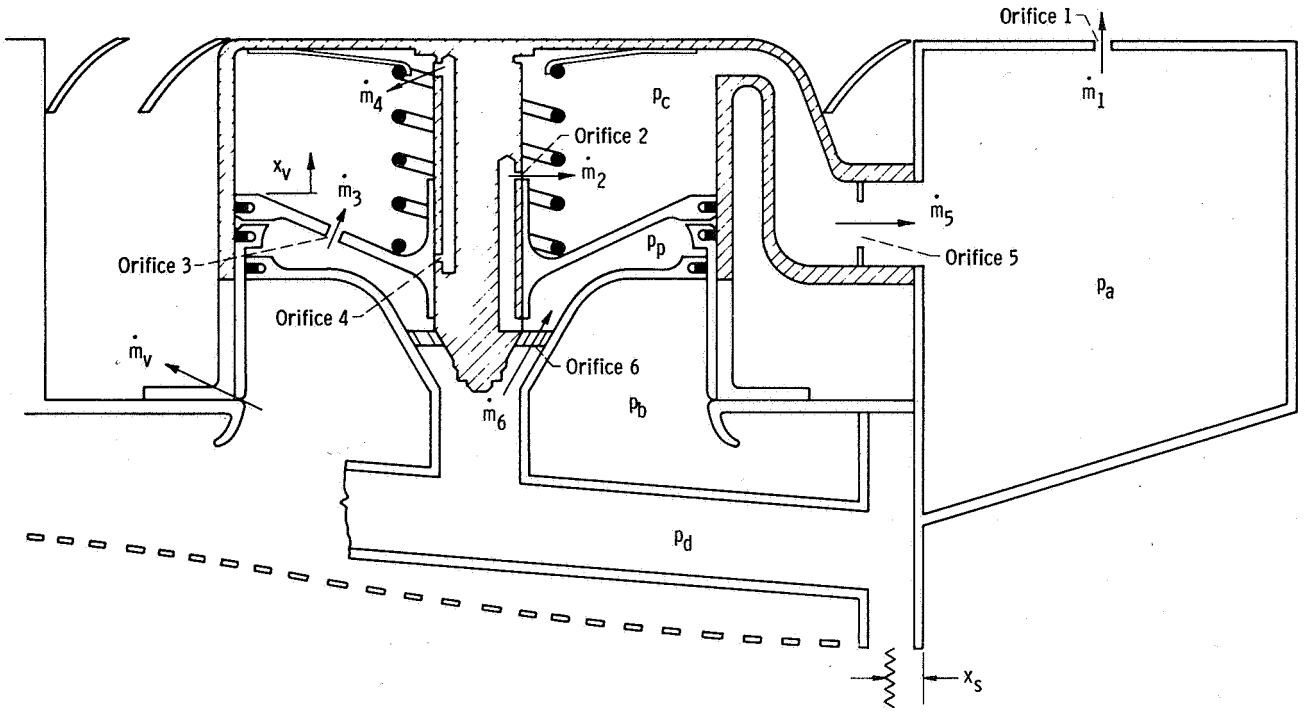

(a) Shielded stability valve with bleed orifices.

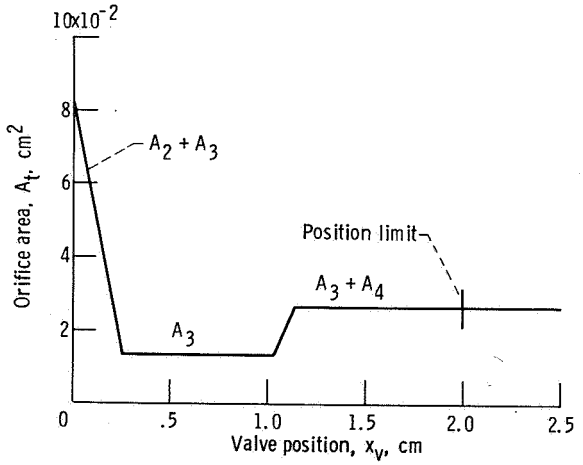

(b) Total bleed orifice areas across poppet.

Figure 7. - Effect of addition of bleed orifices to stability valve.

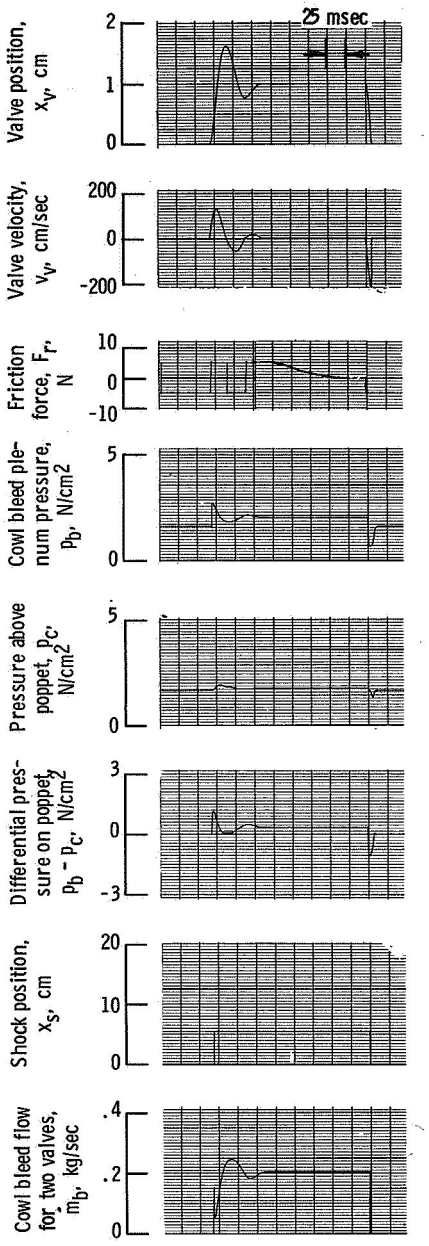

Figure 8. - Typical recording of analog data showing response of stability valve system to a step in shock position. Unshielded valve; friction force, F_r, 4.45 N; damping orifice diameter, D_5, 1.02 cm.

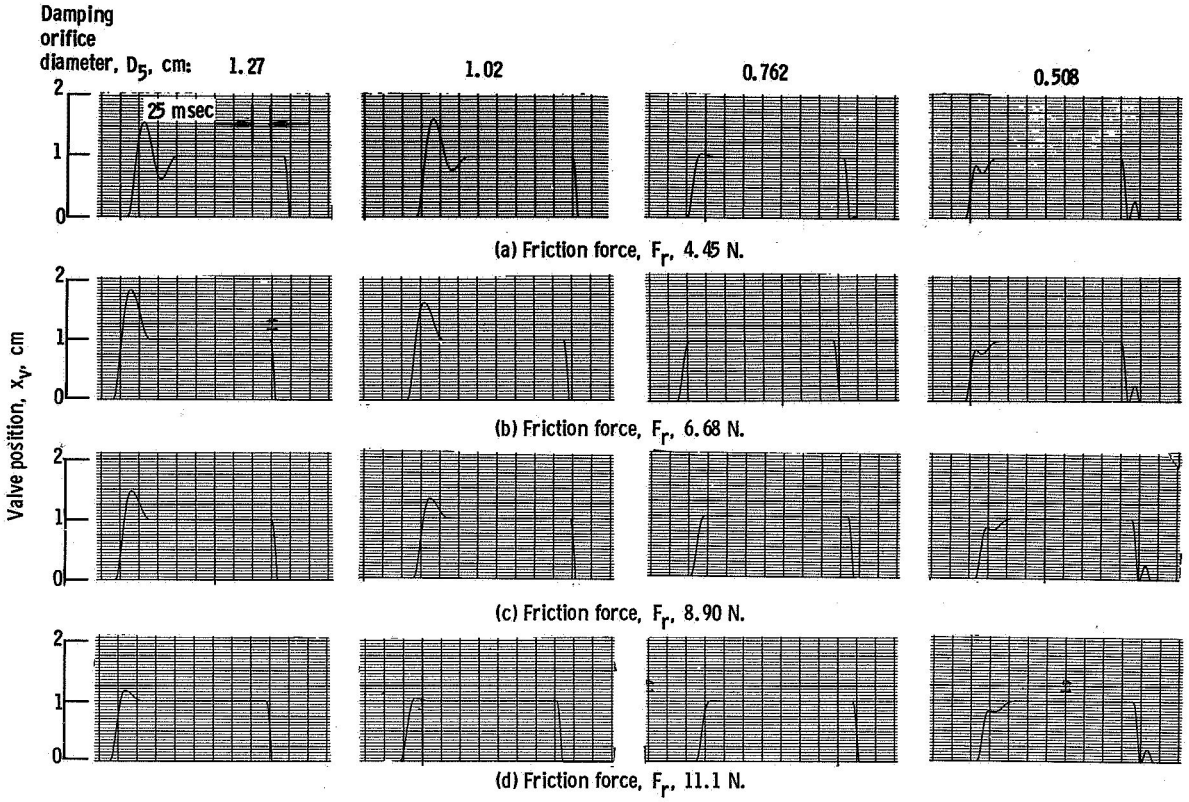

Figure 9. - Effect of friction force and damping orifice diameter on unshielded-stability-valve response to a step in shock position.

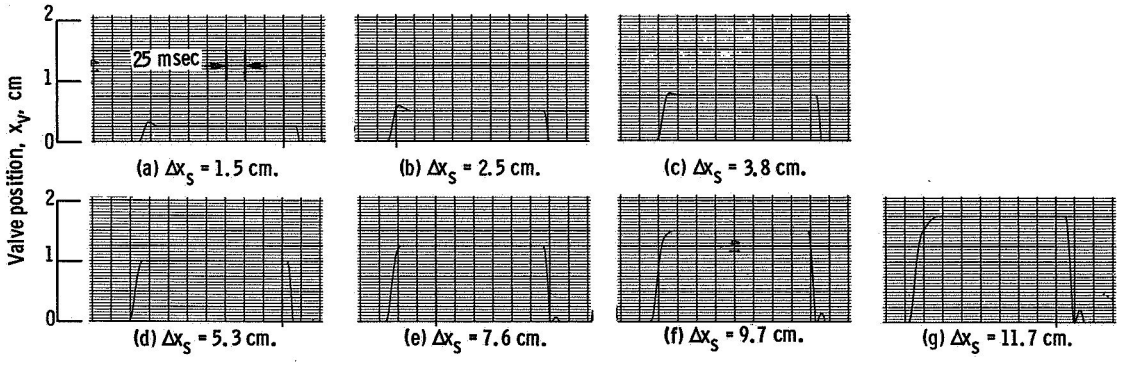

Figure 10. - Effect of step size Δx_s on unshielded-stability-valve response to a step in shock position. Friction force, F_r, 6.68 N; damping orifice diameter, D_5, 0.762 cm.

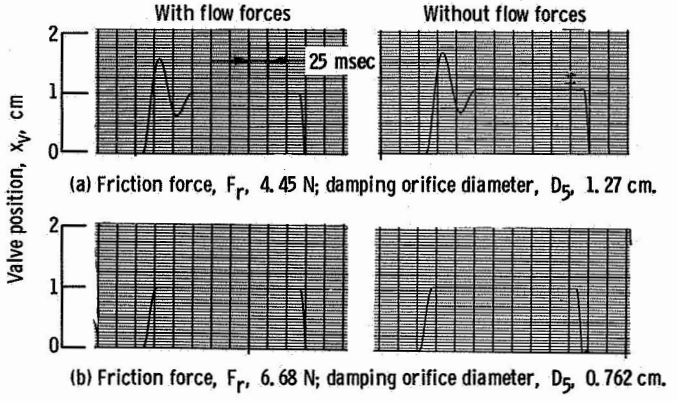

(a) Friction force, F_r, 4.45 N; damping orifice diameter, D_5, 1.27 cm.

(b) Friction force, F_r, 6.68 N; damping orifice diameter, D_5, 0.762 cm.

Figure 11. - Effect of flow forces on two configurations of the unshielded stability valve responding to a step in shock position.

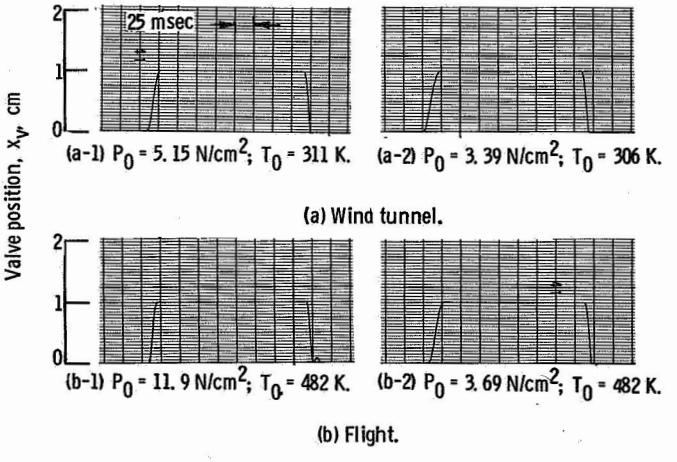

(a-1) P_0 = 5.15 N/cm^2; T_0 = 311 K. (a-2) P_0 = 3.39 N/cm^2; T_0 = 306 K.

(a) Wind tunnel.

(b-1) P_0 = 11.9 N/cm^2; T_0 = 482 K. (b-2) P_0 = 3.69 N/cm^2; T_0 = 482 K.

(b) Flight.

Figure 12. - Effect of varying conditions of free-stream total pressure P_0 and temperature T_0 on unshielded-stability-valve response to a step in shock position for operation at Mach 2.5 in both wind tunnel and flight. Friction force, F_r, 6.68 N; damping orifice diameter, D_5, 0.762 cm.

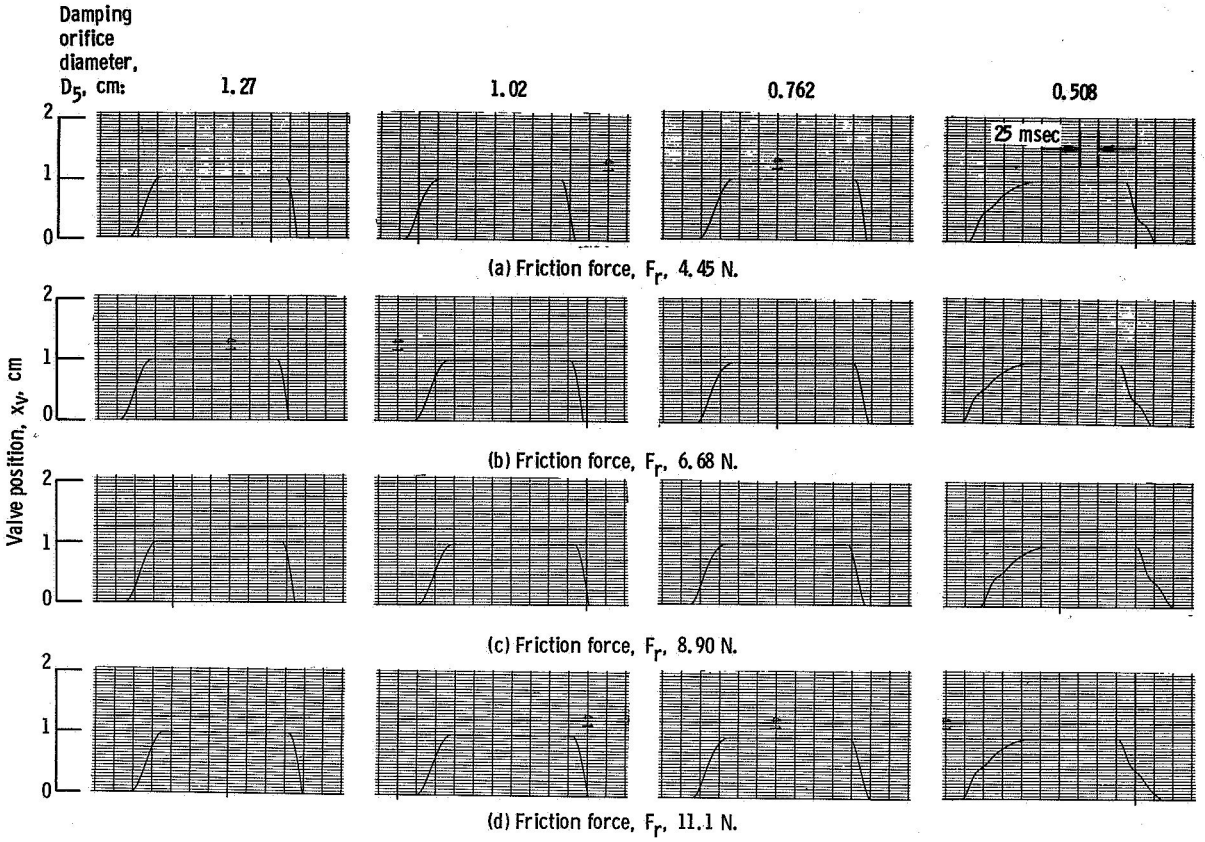

Figure 13. - Effect of friction force and damping orifice diameter on shielded-stability-valve response to a step in shock position.

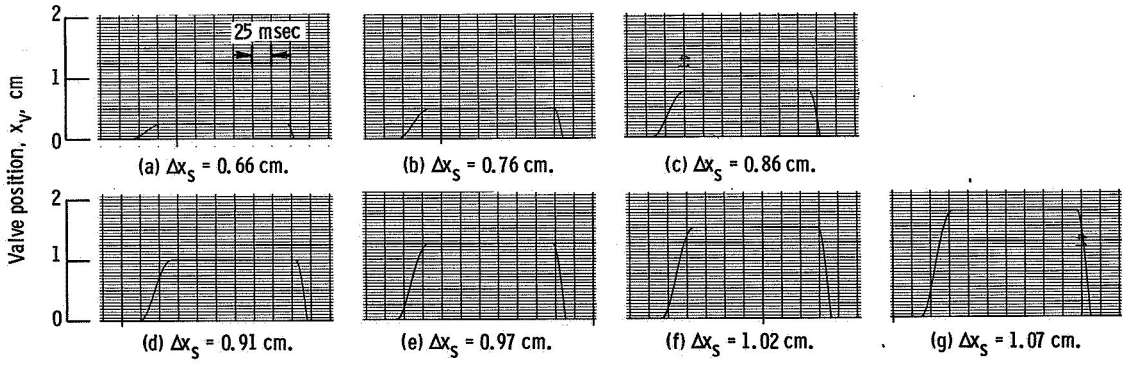

Figure 14. - Effect of step size Δx_s on shielded-stability-valve response to a step in shock position. Friction force, F_r, 4.45 N; damping orifice diameter, D_5, 1.27 cm.

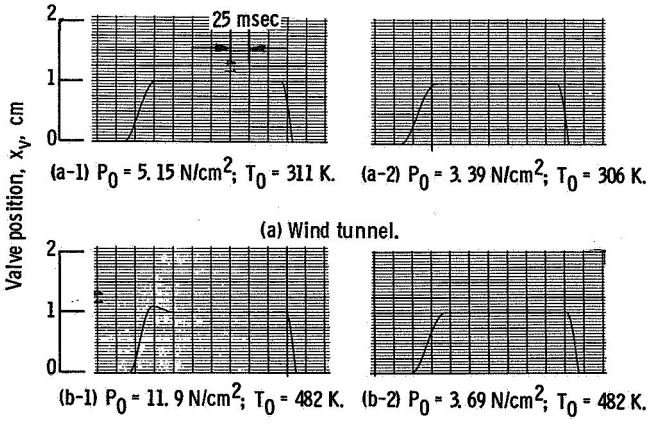

(a-1) P_0 = 5.15 N/cm^2; T_0 = 311 K. (a-2) P_0 = 3.39 N/cm^2; T_0 = 306 K.

(a) Wind tunnel.

(b-1) P_0 = 11.9 N/cm^2; T_0 = 482 K. (b-2) P_0 = 3.69 N/cm^2; T_0 = 482 K.

(b) Flight.

Figure 15. - Effect of varying conditions of free-stream total pressure P_0 and temperature T_0 on shielded-stability-valve response to a step in shock position for operation at Mach 2.5 in both wind tunnel and flight. Friction force, F_r, 4.45 N; damping orifice diameter, D_5, 1.27 cm.

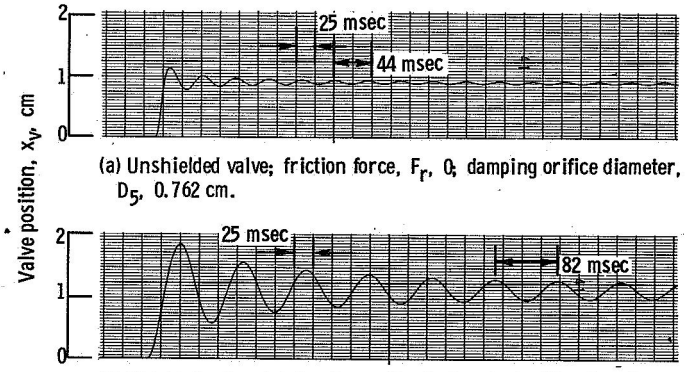

(a) Unshielded valve; friction force, F_r, 0; damping orifice diameter, D_5, 0.762 cm.

(b) Shielded valve; friction force, F_r, 0; damping orifice diameter, D_5, 1.27 cm.

Figure 16. - Response of stability valves to a step in shock position with friction removed from the valve.

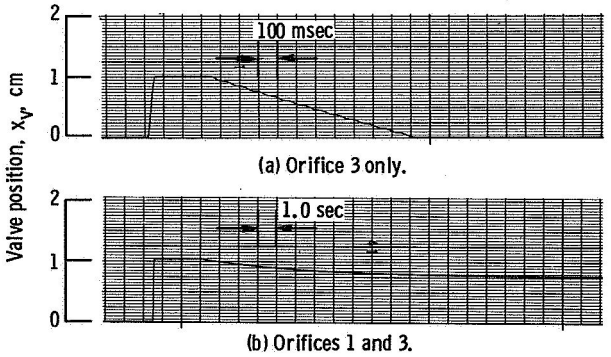

(a) Orifice 3 only.

(b) Orifices 1 and 3.

Figure 17. - Effect of bleed orifices 1 and 3 on response of shielded stability valve to a step in shock position.

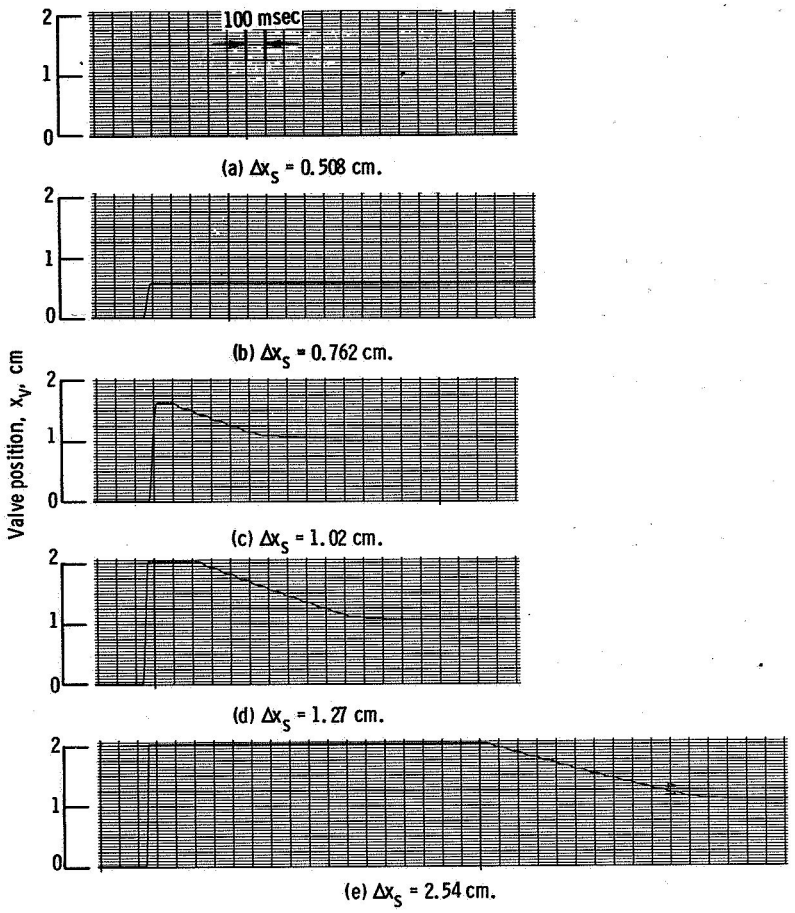

Figure 18. - Response of shielded stability valve to various step sizes in shock position Δx_s with all bleed orifices included.

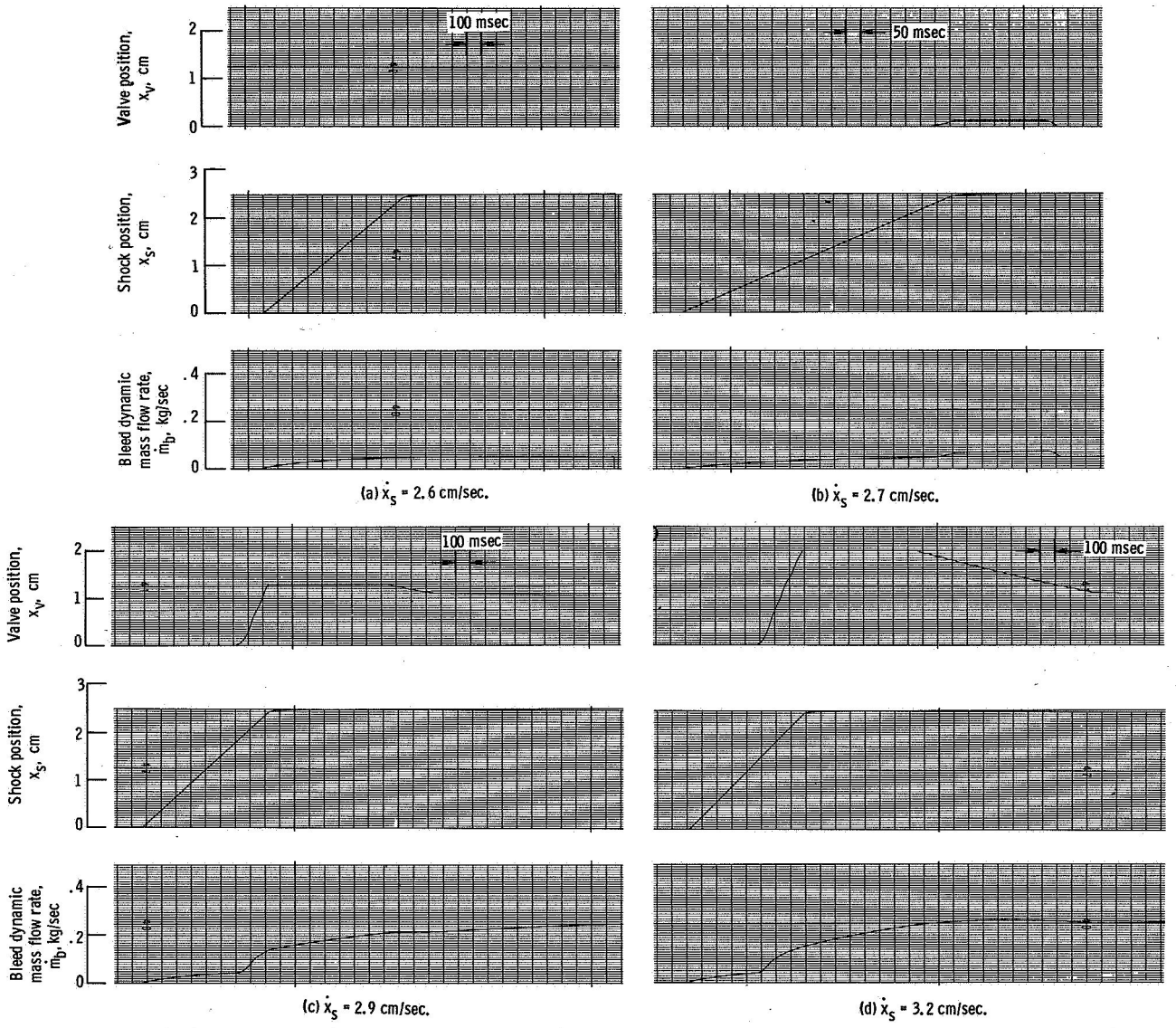

Figure 19. - Response of shielded stability valve to various ramps in shock position x_s with all bleed orifices included. Friction force, F_r, 4.45 N; damping orifice diameter, D_5, 1.27 cm.

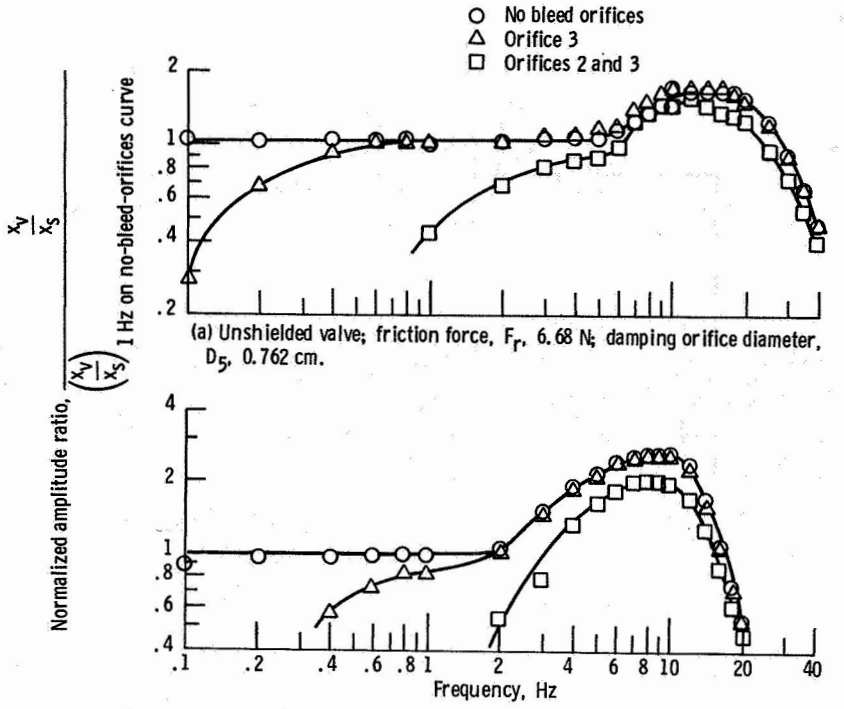

(a) Unshielded valve; friction force, F_r, 6.68 N; damping orifice diameter, D_5, 0.762 cm.

(b) Shielded valve; friction force, F_r, 4.45 N; damping orifice diameter, D_5, 1.27 cm.

Figure 20. - Effect of bleed orifices on frequency response of stability valve.

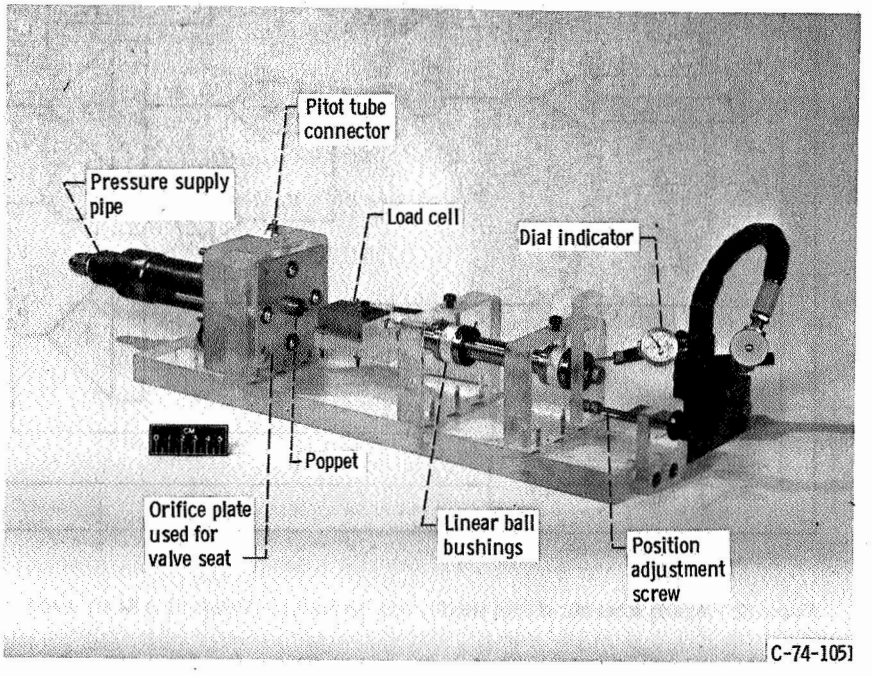

Figure 21. - Test stand for 1/6th-scale model of poppet valve used to determine flow forces and discharge coefficients.

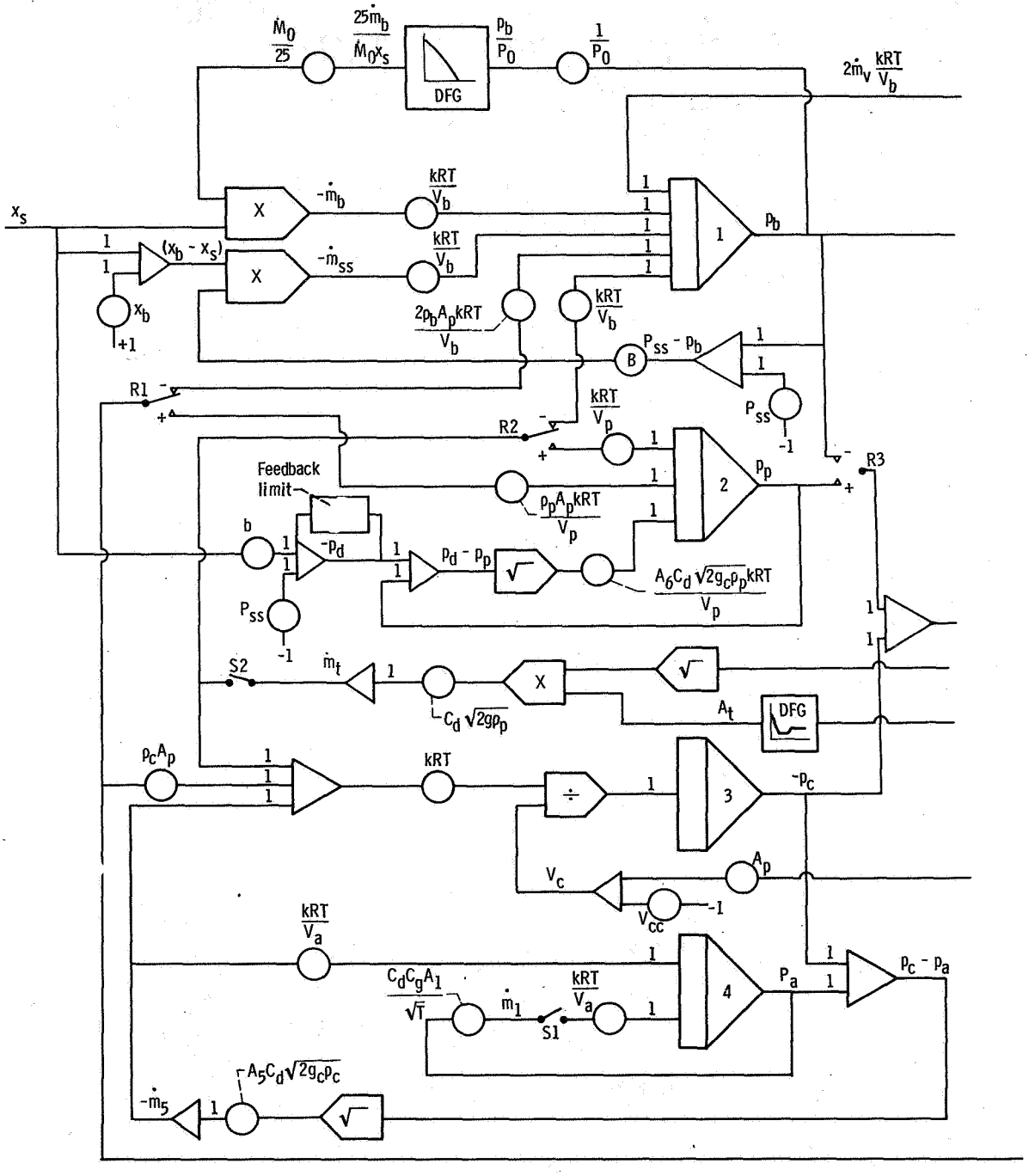

Figure 22. - Analog schematic of inlet stability valve simulation. (Relays R1 to R4 are used to change from unshielded

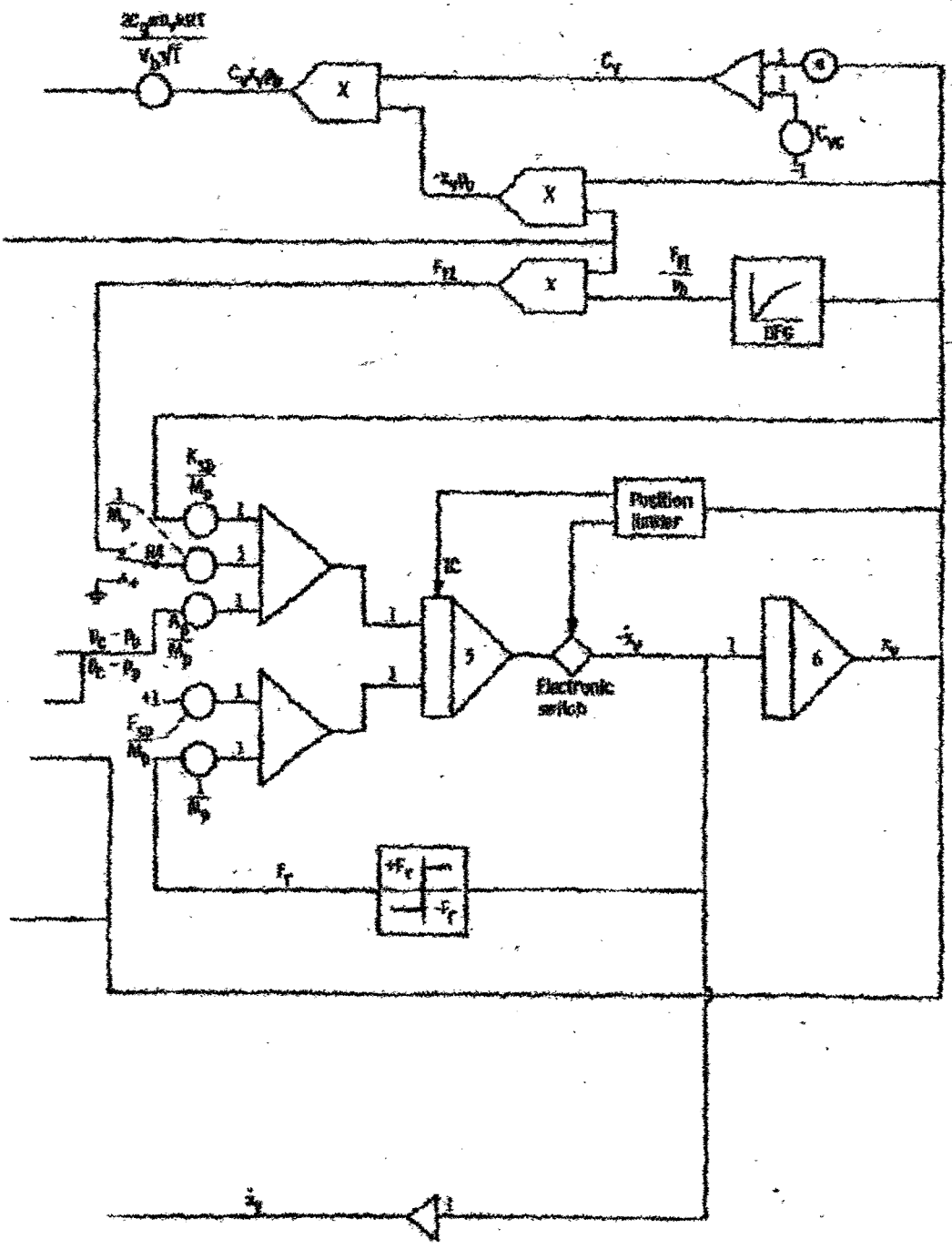

Vad (+) value. Switch S1 removes orifice 1 and switch S2 removes orifices 2, 3, and 4.)

NATIONAL AERONAUTICS AND SPACE ADMINISTRATION
WASHINGTON, D.C. 20546

OFFICIAL BUSINESS
PENALTY FOR PRIVATE USE $300

SPECIAL FOURTH-CLASS RATE
BOOK

POSTAGE AND FEES PAID
NATIONAL AERONAUTICS AND
SPACE ADMINISTRATION
451

U.S. MAIL

POSTMASTER: If Undeliverable (Section 158
Postal Manual) Do Not Return

"The aeronautical and space activities of the United States shall be conducted so as to contribute . . . to the expansion of human knowledge of phenomena in the atmosphere and space. The Administration shall provide for the widest practicable and appropriate dissemination of information concerning its activities and the results thereof."

—NATIONAL AERONAUTICS AND SPACE ACT OF 1958

NASA SCIENTIFIC AND TECHNICAL PUBLICATIONS

TECHNICAL REPORTS: Scientific and technical information considered important, complete, and a lasting contribution to existing knowledge.

TECHNICAL NOTES: Information less broad in scope but nevertheless of importance as a contribution to existing knowledge.

TECHNICAL MEMORANDUMS: Information receiving limited distribution because of preliminary data, security classification, or other reasons. Also includes conference proceedings with either limited or unlimited distribution.

CONTRACTOR REPORTS: Scientific and technical information generated under a NASA contract or grant and considered an important contribution to existing knowledge.

TECHNICAL TRANSLATIONS: Information published in a foreign language considered to merit NASA distribution in English.

SPECIAL PUBLICATIONS: Information derived from or of value to NASA activities. Publications include final reports of major projects, monographs, data compilations, handbooks, sourcebooks, and special bibliographies.

TECHNOLOGY UTILIZATION PUBLICATIONS: Information on technology used by NASA that may be of particular interest in commercial and other non-aerospace applications. Publications include Tech Briefs, Technology Utilization Reports and Technology Surveys.

Details on the availability of these publications may be obtained from:

SCIENTIFIC AND TECHNICAL INFORMATION OFFICE

NATIONAL AERONAUTICS AND SPACE ADMINISTRATION

Washington, D.C. 20546